High-Efficiency X-Band MMIC GaN Power Amplifiers Operating as Rectifiers

Michael Litchfield, Scott Schafer, Tibault Reveyrand, Zoya Popović

University of Colorado at Boulder, Colorado

Abstract—**This paper presents a performance evaluation of GaN X-Band power amplifiers operating as self-synchronous rectifiers. Two single-stage MMIC power amplifiers are characterized under continuous wave conditions at 10.1 GHz. One PA is designed with a single $10 \times 100\mu$m HEMT in a 0.15μm GaN process, while the other contains two $10 \times 100\mu$m power-combined devices. The MMICs exhibit 67% and 56% power added efficiency at $V_{DD} = 20$ V in deep class-AB bias, respectively. In rectifier mode, biased in class-C, the same MMICs show a RF-to-DC efficiency of 64%. The output powers of the two MMIC PAs are around 3.2W. In rectifier mode, the gate DC bias and the load-pull determined RF gate impedance are set for optimal efficiency. The DC load does not affect the efficiency substantially, and can be chosen for a desired voltage or current. The paper demonstrates that high-power efficient GaN rectifiers can be achieved by designing high-efficiency PAs at least up to X-band.**

Index Terms—**MMIC, power amplifiers, gallium nitride, rectifier.**

I. INTRODUCTION

Microwave rectifiers have applications in wireless power transmission where they are integrated with antennas, e.g. [1]–[3], as well as outphasing amplifiers with energy recycling [4]–[6]. These rectifiers are designed typically with Schottky diodes, which have limited power handling capability. Recently, advanced DC/DC converters have been demonstrated in the UHF frequency range with transistor rectifiers, scaled from low-frequency synchronous rectifier architectures [7], [8]. It has recently also been shown theoretically as well as experimentally at 2 GHz that a microwave transistor, when load impedances are well matched, can exhibit similar efficiency when operating either as a power amplifier or a rectifier, as a results of time-reversal duality [9], [10].

In this paper, two high-efficiency X-Band GaN MMIC power amplifiers are investigated for rectifying purposes. First, the PAs are characterized in large signal, at 10.1 GHz and with $V_{DD} = 20$ V in order to evaluate their DC-to-RF efficiency (Power Added Efficiency). Then, they are measured as self-synchronous rectifiers, where the RF signal is injected into the drain RF port with the drain bias replaced by a DC load. The output is then the drain DC port, loaded with an optimal resistor. The gate DC port voltage forces the rectifier bias point into an efficient class-C operating condition. Such a self-synchronous rectifier does not require any RF gate input signal, since the finite gate-to-drain nonlinear capacitance (C_{gd}) in the intrinsic GaN HEMT provides feedback and allows the transistor to generate RF power at the gate port. The best efficiency is obtained when the gate RF port is terminated in an optimal passive RF complex load.

The MMICs are designed in a 0.15μm gate length TriQuint GaN on SiC process, with output matching optimized for high efficiency at X-band. Fig. 1 shows the X-Band power amplifier MMICs characterized in both amplifier and rectifier modes in this paper:

- Circuit-A (Fig. 1a) is a $10 \times 100\mu$m single transistor amplifier;
- Circuit-B (Fig. 1b) is a single stage amplifier that combines two $10 \times 100\mu$m transistors with a reactive non-isolated combiner, with a single gate and drain bias connection.
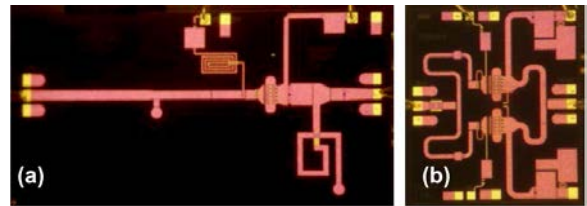

Fig. 1. X-Band MMIC power amplifiers operated as rectifiers. (a) Circuit-A: single-stage single-ended PA, using a $10 \times 100\mu$m transistor. The die is 3.8×2.3mm^2 in size. (b) Circuit-B: single-stage power combined PA, with two $10 \times 100\mu$m transistors, and an overall footprint of 2.0×2.3mm^2.

II. MEASUREMENT SETUP

The measurement setup is based on a 4-channel time-domain receiver, operating as a large signal network analyzer (LSNA) [11]. Bi-directional couplers are implemented in the instrument to acquire absolute incident and reflected waves at the DUT's input and output ports. A relative SOLT calibration associated with a power calibration, enables accurate measurements of time-domain RF waveforms for voltages and currents at the calibration reference planes [12]. The LSNA enables measurements in a 30 GHz RF bandwidth, and therefore only the 10-GHz fundamental and the second harmonic frequencies are measured. However, in the context of this paper, the most relevant information is at the fundamental frequency and at DC.

For the power amplifier measurements, the RF input signal is at the gate and both RF ports are terminated in 50 Ω. The DC-to-RF efficiency is calculated as both the power-added and the drain efficiency, defined by:

$$ PAE = \frac{P_{out}(f_0) - P_{in}(f_0)}{P_{DC}} \; ; \; \eta_{DE} = \frac{P_{out}(f_0)}{P_{DC}} \qquad (1) $$
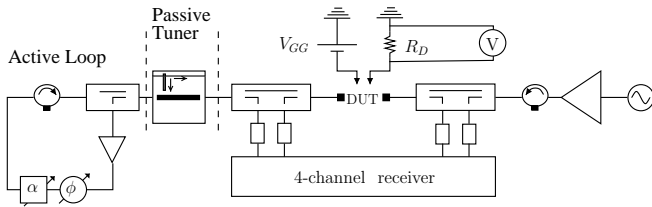
Fig. 2. Time-domain measurement setup for rectifier characterization. A load-pull is performed at the gate RF port of the DUT, with a passive tuner and an active loop that enables a highly reflective load impedance at 10.1 GHz.

Regarding the rectifier characterization, the RF signal is injected at the RF drain port of the DUT. The output of the rectifier is at the drain DC path, and only the gate of the transistor is biased. In order to obtain the best efficiency, the DC load at the drain (R_D) and RF load at the gate, are both varied as depicted in Fig. 2. The load-pull is performed at the fundamental frequency (10.1 GHz) with a passive tuner. The active loop shown in the figure enables a high magnitude of the reflexion coefficient presented to the gate port. The RF-to-DC or rectifier conversion efficiency is given by :

$$\eta_R = \frac{P_{DC}}{P_{RF\,injected}} = \frac{2|V_{DC}|^2}{RD \times \Re\{V_{drain}(f_0)\,I^*_{drain}(f_0)\}} \quad (2)$$

For the presented data, the MMICs are mounted in a coaxial test fixture. The error-boxes of the test-fixture are extracted with a TRL calkit. The data given is this paper are de-embedded to the input and output GSG ports pictured on Fig. 1.

III. MEASURED RESULTS

A. Circuit-A: single-ended PA

Circuit-A, operating as an amplifier in a 50-Ω environment is measured at $f_0 = 10.1$ GHz, and exhibits a peak efficiency of $PAE = 67.87\%$ and $\eta_{DE} = 78.36\%$ with $P_{in} = 26.42$ dBm and $P_{out} = 35.16$ dBm, as shown in Fig. 3. The bias point of $V_{GG} = -4.0$ V and $V_{DD} = 20$ V is optimized for an operating condition close to class-B.
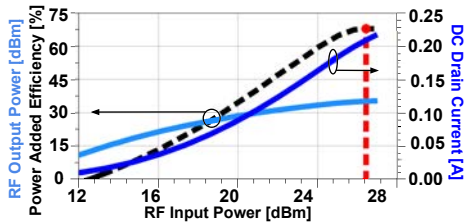

Fig. 3. Circuit-A best efficiency performance as an amplifier is measured with $V_{GG} = -4.0$ V and $V_{DD} = 20$ V. Light blue curve is the output power, dark blue is the DC drain current and the efficiency (PAE) is traced with a black dashed line. The maximum efficiency is $PAE = 67.87\%$ at $P_{in} = 26.42$ dBm (red dashed line).

This circuit has been characterized as a rectifier with the bench depicted in Fig. 2. In order to optimize the RF-to-DC efficiency (η_R), we can adjust 3 parameters: the gate bias voltage (V_{GG}), the DC load impedance at the output (R_D)

and the RF load impedance on the gate (Z_{load} or Γ_{load}), as discussed below.

- **$\mathbf{Z_{load}}$** is of prime importance regarding conversion efficiency of the circuit.
- **$\mathbf{V_{GG}}$** should correspond to a class-B or class-C condition to ensure that the transistor operates in rectifier mode. V_{GG} has a moderate influence on the efficiency compared to Z_{load}. In this work, we noticed that a deep class-C bias point makes it possible to reach the best efficiency. Fig. 4 illustrates a V_{GG} sweep for fixed Z_{load} and R_D. An $\eta_R = 60.37\%$ has been measured at $P_{RF} = 34.63$ dBm but in this case, Z_{load} is not optimized and is limited by the passive tuner X-band SWR range during our automated multi-sweep measurements).
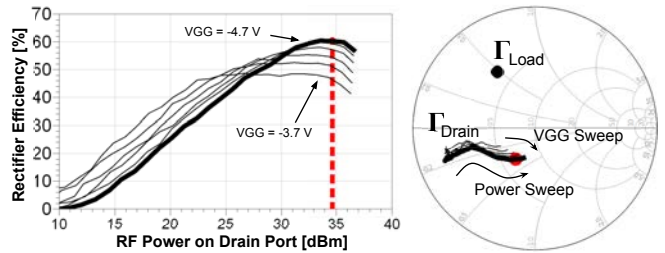

Fig. 4. Circuit-A rectifying performance for V_{GG} between -3.7 V and -4.7 V with a 0.2 V step). The gate RF port is terminated at the fundamental frequency with $Z_{load} = (17.9 + j\,24.0)\Omega$ and the drain DC load impedance is $R_D = 100\Omega$.

- The range of **$\mathbf{R_D}$** should be limited during the measurements to the DC voltage and current values the transistor can handle. The value of R_D can be chosen to increase either voltage or current, since the efficiency as defined in (2) does not vary appreciably with the DC load resistance. However, the value of R_D impacts the RF impedance at the input of the rectifier (drain RF port).
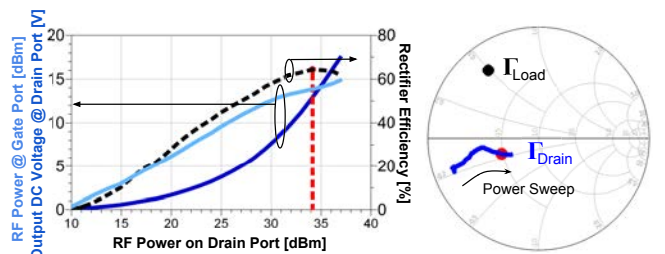

Fig. 5. Circuit-A: Rectifier efficiency η_R (black dashed line), DC output drain voltage (dark blue) and RF power at the gate reference plane (light blue) versus injected drain RF power. The best rectifying performance is $\eta_R = 64.4\%$ at $P_{RF} = 34.14$ dBm (red dashed line). The Smith chart on the right shows the optimal load impedance presented at the gate port (black dot) and the drain impedance of the DUT (blue curve) during the power sweep.

After optimization of Z_{load}, R_D and V_{GG} in circuit-A, the best rectifying efficiency $\eta_R = 64.40\%$ is obtained at $V_{GG} = -4.7$ V, $R_D = 100\Omega$ and $Z_{load} = (8.45 + j\,24.5)\Omega$. The RF power sweep results are depicted in Fig. 5. The higher value of Z_{load} in this case is enabled by the active loop. The RF power measured at the gate reference plane is also displayed and

demonstrates the fact that the PA can operate as an efficient self-synchronous rectifier thanks to a passive load applied at the gate RF port.

B. Circuit-B: power-combined MMIC

Circuit-B has been characterized in the same manner as circuit-A for both amplifier and rectifier modes of operation. Regarding the amplifier measurements, with a $50\,\Omega$ load, at $10.1\,\text{GHz}$, circuit B exhibits the best efficiency $PAE = 56.47\%$ and $\eta_{DE} = 65.75\%$ with $P_{in} = 26\,\text{dBm}$ and $P_{out} = 35\,\text{dBm}$. The bias point is $V_{GG} = -3.4\,\text{V}$ and $V_{DD} = 20\,\text{V}$. The design of the amplifier is optimized for a deep class-AB bias.
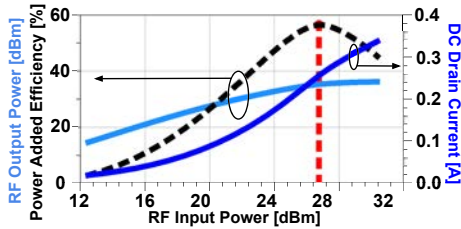

Fig. 6. Circuit-B as an amplifier: PAE (black dashed line), output RF power (light blue) and DC drain current (dark blue) versus input RF power. The best efficiency is $PAE = 56.47\%$ at $P_{in} = 26\,\text{dBm}$ (red dashed line) with $V_{GG} = -3.4\,\text{V}$, $V_{DD} = 20\,\text{V}$.

Rectifier measurements have been performed on circuit-B after optimization of the variables Z_{load}, R_D and V_{GG}. This HEMT PA-based rectifier is 63.94% efficient. Once again, Z_{load} has been enabled by the active loop depicted on Fig. 2. The measured RF power sweep is shown in Fig. 7. As was shown with Circuit-A, we notice that the RF power at the gate port (light blue line) makes it possible to find a specific passive impedance that results in high rectifying efficiency.
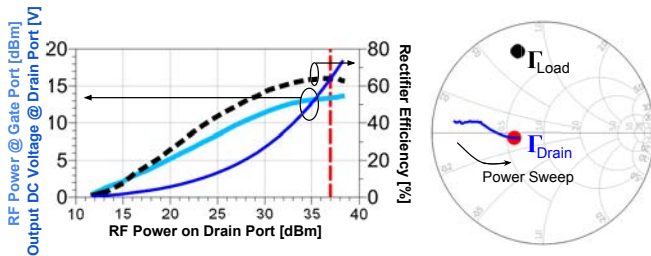

Fig. 7. Circuit-B best rectifying performances with $V_{GG} = -4.7\,\text{V}$, $R_D = 80\,\Omega$ and a RF impedance load applied at the gate port $Z_{load} = (9.8 + j\,35.75)\,\Omega$. The circuit exhibits a rectification efficiency $\eta_R = 63.94\%$ with $37\,\text{dBm}$ RF power injected into the drain port. RF power at the gate port (light blue), output DC voltage (dark blue) and rectifying efficiency (black dash) are displayed on the left. The plot on the right displays the rectifier input impedance Γ_{Drain} (drain port) and load impedance Γ_{Load} (gate port).

Finally, Table I summarizes performances of the two X-band GaN MMICs for both amplifier and rectifier operation modes. In the case of amplifier mode, PAE is displayed *efficiency*. The *RF power* is the power at the drain RF port. By demonstrating high efficiency even at X-Band, this work highlights the possibility of using GaN HEMTs for designing

both single-ended and power combined rectifiers. For the power combined rectifier, the DC combining efficiency from Table I is 80% in this case, since the devices are all of equal size and are measured with the same gate bias.

Since a nonlinear transistor model that is valid for both amplification and rectification modes is not available for most devices, there is a need for nonlinear models which contain, for example, intrinsic nonlinear capacitances extracted from first and third quadrants of the I-V curves.

TABLE I
PERFORMANCES AS AMPLIFIER AND RECTIFIER AT 10.1 GHZ

Circuit	Amplifier		Rectifier	
	A	B	A	B
Max Efficiency(%)	67.87	56.47	64.40	63.94
DC Power (mW)	4186	5112	1671	3182
RF Power (mW)	3281	3362	2594	4976

IV. CONCLUSION

This work shows measured results on two X-Band GaN MMICs fabricated in the $0.15\,\mu\text{m}$ process and operated in both amplifier and rectifier modes. High efficiencies are obtained for both amplification and rectification modes. Rectification is performed in a self-synchronous way without any RF input at the gate port. A passive termination at the gate is self-sufficient at microwave frequencies due to the feedback produced by C_{gd} in the HEMT GaN intrinsic non-linear model.

ACKNOWLEDGMENT

REFERENCES

[1] J. O. McSpadden, L. Fan, and K. Chang, "Design and experiments of a high-conversion-efficiency 5.8-ghz rectenna," *Microwave Theory and Techniques, IEEE Transactions on*, vol. 46, no. 12, pp. 2053–2060, 1998.

[2] N. Shinohara and H. Matsumoto, "Experimental study of large rectenna array for microwave energy transmission," *Microwave Theory and Techniques, IEEE Transactions on*, vol. 46, no. 3, pp. 261–268, 1998.

[3] Z. Popović, "Cut the Cord: Low-Power Far-Field Wireless Powering," *IEEE Microwave Magazine*, vol. 14, no. 2, pp. 55–62, Mar. 2013.

[4] R. Langridge, T. Thornton, P. Asbeck, and L. Larson, "A power re-use technique for improved efficiency of outphasing microwave power amplifiers," *IEEE Transactions on Microwave Theory and Techniques*, vol. 47, no. 8, pp. 1467–1470, 1999.

[5] P. Godoy, D. Perreault, and J. Dawson, "Outphasing Energy Recovery Amplifier With Resistance Compression for Improved Efficiency," *IEEE Transactions on Microwave Theory and Techniques*, vol. 57, no. 12, pp. 2895–2906, Dec. 2009.

[6] J. Xu and D. S. Ricketts, "An Efficient, Watt-Level Microwave Rectifier Using an Impedance Compression Network (ICN) With Applications in Outphasing Energy Recovery Systems," *IEEE Microwave and Wireless Components Letters*, vol. 23, no. 10, pp. 542–544, Oct. 2013.

[7] J. A. Garcia, R. Marante, and M. de las Nieves Ruiz Lavin, "GaN HEMT Class E^2 Resonant Topologies for UHF DC/DC Power Conversion," *IEEE Transactions on Microwave Theory and Techniques*, vol. 60, no. 12, pp. 4220–4229, Dec. 2012.

[8] J. A. García, R. Marante, M. N. Ruiz, and G. Hernández, "A 1 GHz Frequency-Controlled Class E 2 DC / DC Converter for Efficiently Handling Wideband Signal Envelopes," in *IEEE MTT-S Digest, IMS 2013*, Seattle, WA, 2013, pp. 1–4.

[9] M. Roberg, T. Reveyrand, I. Ramos, E. A. Falkenstein, and Z. Popović, "High-Efficiency Harmonically Terminated Diode and Transistor Rectifiers," *IEEE Transactions on Microwave Theory and Techniques*, vol. 60, no. 12, pp. 4043–4052, Dec. 2012.

[10] T. Reveyrand, I. Ramos, and Z. Popović, "Time-reversal duality of high-efficiency RF power amplifiers," *Electronics Letters*, vol. 48, no. 25, pp. 1607–1608, Dec. 2012.

[11] P. Roblin, *Nonlinear RF circuits and nonlinear vector network analyzers*. Cambridge University Press, 2011.

[12] J. Verspecht, "Calibration of a measurement system for high frequency nonlinear devices," *Brussels, Belgium Vrije Univeriteit Brussels, Ph. D. Thesis*, 1995.